ACCSCIENCE PUBLISHING

Asian Journal of Water, Environment and Pollution

ORIGINAL RESEARCH ARTICLE

Sustainable removal of Pb(II), Zn(II), and Ni(II) from aqueous solutions using date-pit-derived biochar: Performance evaluation under batch conditions

Marwa Y. Khudair[1]*, Rajaa N. Al-Yassein[2], and Nawras A. Al-Faiz[3]

[1]Soil & Water Resources Department, College of Agriculture, University Of Anbar, Ramadi, Iraq

[2]Department of Pathological Analyses, College of Science, University of Basrah, Basrah, Iraq

[3]Department of Natural Marine Science, College of Marine Sciences, University of Basrah, Basrah, Iraq

Abstract

Heavy metal contamination in water remains a persistent environmental concern, particularly in regions where access to advanced treatment technologies is limited. In this study, biochar produced from date pits, an agricultural waste material, was investigated as a low-cost adsorbent for the removal of Pb(II), Zn(II), and Ni(II) from aqueous solutions. Batch experiments were conducted to evaluate the effects of contact time (5–120 min), solution pH (3–9), and initial metal concentration (5–50 mg L^{-1}). The results showed that adsorption equilibrium was reached within 60 min for all metals. The maximum adsorption capacities were 39.6 mg g^{-1} for Pb(II), 23.5 mg g^{-1} for Zn(II), and 21.0 mg g^{-1} for Ni(II) at pH 7. Adsorption increased with increasing pH, and the affinity followed the order Pb(II) > Zn(II) > Ni(II), likely due to differences in hydration energy and interaction with surface functional groups. Kinetic analysis indicated that the adsorption process followed a pseudo-second-order model, while the equilibrium data were best described by the Langmuir isotherm model, suggesting monolayer adsorption behavior. Overall, the findings indicate that date-pit-derived biochar can serve as an effective and accessible material for removing divalent heavy metals from water, with potential application in simple and decentralized treatment systems.

Keywords: Biochar; Date pits; Heavy metals; Adsorption; Aqueous medium

***Corresponding author:**
Marwa Y. Khudair
(ag.marwa.yass@uoanbar.edu.iq)

Citation: Khudair MY, Al-Yassein RN, Al-Faiz NA. Sustainable removal of Pb(II), Zn(II), and Ni(II) from aqueous solutions using date-pit-derived biochar: Performance evaluation under batch conditions. *Asian J Water Environ Pollut.* 2026;23(4):026140095. doi: 10.36922/AJWEP026140095

Received: April 2, 2026

Revised: May 3, 2026

Accepted: May 11, 2026

Published online: June 16, 2026

1. Introduction

Due to the accelerating pace of industrialization as well as urban and agricultural development, heavy metal contamination in groundwater has emerged worldwide as a prominent problem.[1] Effluents, untreated or poorly treated, routinely emptied into rivers, irrigation channels, and shallow groundwater aquifers are responsible for the accumulation of toxic metals in the aquatic ecosystems in many developing countries.[2] Of these contaminants, cadmium (Cd), lead (Pb), zinc (Zn), and nickel (Ni) constitute a major pollution threat because they persist in the environment over time, are toxic, and bioaccumulate in living organisms.[3] Extended contact with these metals

is correlated with neurological illnesses, renal injury, developmental disorders, and lower agricultural efficiency, even at low levels.[4,5] Heavy metal contamination is a major concern because these pollutants can bioaccumulate and biomagnify through aquatic food webs[6], making them long-term environmental and human health concerns. In this sense, a policy that reduces heavy metal flows to water bodies forms part of broader medium- and long-term strategies for protecting aquatic environments and human health.[7]

Common approaches to heavy metal separation from industrial wastewater, such as chemical precipitation, ion exchange, membrane filtration, and electrochemical treatments, are characterized by high operational costs and energy demand, an important issue when the generation of secondary waste that requires additional treatment is also considered. These limitations have driven a growing interest in alternative remediation methods that are low-cost, accessible locally, and environmentally benign.[2]

In this context, biochar has attracted considerable attention as a promising adsorbent due to its porous structure, relatively large surface area, and the presence of functional groups capable of binding metal ions through electrostatic attraction, complexation, and ion-exchange mechanisms.[8,9] Recent reviews have documented the value of biochar from cheap biomass as a sustainable material for wastewater treatment by its adsorption, ion exchange, and surface complexation mechanisms to restore soil properties. Nevertheless, the results are feedstock type-, pyrolysis conditions-, surface chemistry-, and regeneration efficiency-dependent, narrowing its large-scale application.[10,11] Biochar is typically produced through the pyrolysis of agricultural residues under limited oxygen conditions, and its physicochemical properties strongly depend on the type of feedstock and the operating temperature used during its production.[12]

Numerous studies have demonstrated the effectiveness of biochars derived from feedstocks such as rice husk, coconut shell, and wood waste for the removal of heavy metals from aqueous solutions. However, comparatively less attention has been given to the adsorption behavior of biochar derived from date pits, despite their availability in large quantities in Middle Eastern countries.[2,13] Iraq, in particular, is one of the leading producers of dates worldwide, generating substantial amounts of date pits as agricultural waste that are often discarded without beneficial use.[14] Converting this biomass into biochar not only represents an environmentally sound waste management strategy but also provides a sustainable and low-cost material for local water treatment applications.

Biochar generated from date pits offers a viable solution as water stress increases and inexpensive remediation technologies become increasingly necessary in these arid and semi-arid regions.[12,15] However, systematic studies on the adsorption kinetics, equilibrium behavior, and factors governing the removal of Pb(II), Zn(II), and Ni(II) ions by date-pit-derived biochar under batch conditions are still scarce.[4] Furthermore, while a number of early studies employed sophisticated analytical methodologies, fewer investigations have focused on the applicability of benchtop methods, e.g., colorimetric ones, which are more appropriate for resource-limited laboratories.

Thus, the present study investigates the adsorption of Pb(II), Zn(II), and Ni(II) ions from aqueous solutions onto biochar prepared by pyrolysis in a muffle furnace. The interaction time, pH of solution, and initial concentration of metal were studied, and adsorption kinetics and equilibrium isotherm models were applied to obtain a deeper understanding of the adsorptive behavior as well as to estimate the sorption capacity of the prepared biochar.

2. Materials and methods

2.1. Preparation of biochar

Date pits were washed with distilled water to remove dust and surface impurities, and then oven-dried at 105 °C for 24 h, and residual pulp and surface impurities were removed from the date pits. After drying, a muffle furnace (L 9/11, Nabertherm GmbH, Germany) was used for pyrolysis at 450 °C for 1 h under anaerobic conditions. The resulting biochar was ground and sieved to pass through a 2-mm pore size. The sieved biochar was then washed with deionized water to remove the soluble ash fraction and dried again before being used in adsorption experiments.[16] The preparation conditions were selected in line with previous reports showing that pyrolysis temperature, heating conditions, and feedstock properties strongly influence biochar yield, porosity, surface functional groups, and adsorption performance.[17]

2.2. Fourier transform infrared spectroscopy

The surface functional groups of the studied date-pit-derived biochar were confirmed by Fourier transform infrared (FTIR) spectroscopy. The FTIR spectrum was recorded on a Bruker FT-IR spectrometer (Tensor 27, Germany) with an attenuated total reflectance (ATR) accessory. Spectra were collected between 4,000 cm^{-1} and 500 cm^{-1} with a resolution of 4 cm^{-1}, by averaging 32 scans at room temperature. The FTIR analysis was used to determine the chemical groups that were responsible for the adsorption of Pb(II), Zn(II), and Ni(II) ions on the biochar surface.

2.3. Determination of the pH point of zero charge

The pH point of zero charge (pHpzc) of date-pit-derived biochar was found by using the pH drift method in order to evaluate the surface charge behavior of the adsorbent. A 50 mL aliquot of 0.01 M NaCl was used as the background electrolyte to control ionic strength. The initial pH (pHi) of each solution was adjusted from 2 to 12 with 0.1 M HCl or 0.1 M NaOH. Then, 0.05 g of biochar was added to each flask, and the suspensions were shaken mechanically for 24 h at room temperature for equilibrium between the solid and liquid phases.

The final pH (pHf) of each suspension was measured using a calibrated pH meter after equilibration. The ΔpH was determined as (pHf – pHi). The pHpzc was calculated by the intersection of the ΔpH versus pHi plot, where ΔpH = 0; this value was defined as the pH at which the biochar surface has no net charge.

2.4. Preparation of metal solutions

Lead nitrate ($Pb(NO_3)_2$), zinc nitrate ($Zn(NO_3)_2$), and nickel nitrate ($Ni(NO_3)_2$) were purchased in analytical grade for stock solutions of each of these metals. Fresh solutions at concentrations of 5–50 mg/L were prepared from stock solutions by diluting the required volume with distilled water prior to each set of experiments.[17]

2.5. Batch adsorption experiments

All adsorption studies were performed using 50 mL of aqueous metal solution in 100 mL Erlenmeyer flasks. Unless otherwise mentioned, 0.05 g of date-pit-derived biochar was added to the flasks for each experiment. The suspensions were shaken in a mechanical shaker at 150 rpm and room temperature (25 ± 2 °C) to ensure uniform mixing of biochar particles with the solution. The experimental set-up was designed to investigate the effects of contact time, solution pH, and initial metal concentration on removal efficiency using the prepared biochar for Pb(II), Zn(II), and Ni(II) in a batch system.[18] The range of concentrations chosen was designed to encompass higher contamination situations and to generate a quantifiable adsorption reaction during laboratory batch testing conditions. Pb, Zn, Ni, and other metals were previously detected in river waters from local monitoring studies within Iraq, and the importance of using appropriate indices and treatment methods for evaluating heavy-metal pollution has been discussed.[19]

2.6. Effect of contact time

For the adsorption kinetic assessment, 20 mg/L of Pb(II), Zn(II), and Ni(II) solutions were brought in contact with 0.05 g biochar at pHi of 7. The suspensions were stirred at various times between 5 and 120 min. The suspensions were filtered, and the remaining metal concentrations were analyzed after each time course.

2.7. Effect of pH

The pH of the solution for metal adsorption was tested by adjusting the pHi of 20 mg/L metal solutions to 3, 5, 7, and 9 using either HCl or NaOH. The contact time for the experiments was 60 min, and 0.05 g of biochar was added.

2.8. Adsorption isotherms

Equilibrium adsorption process was carried out at the optimal pH and contact time with the initial metal concentrations of 5–50 mg/L, then the residual metal concentrations were determined, and the Langmuir and Freundlich isotherm models were used to describe equilibrium data.

2.9. Colorimetric determination

The residual Pb(II), Zn(II), and Ni(II) were determined colorimetrically after complexation with dithizone, zincon, and dimethylglyoxime, respectively. The metal contents were determined with a calibrated colorimeter (the calibration curves for all metals had R^2 values of ≥0.995). Each metal was measured individually with its specific colorimetric reagent, and calibration for each analyte was performed so as to minimize potential analytical interferences. Such calibration and analyte-specific measurements were used to minimize potential analytical interferences, as significant heavy-metal determination can be affected by overlapping responses and interferences due to matrix effects, which are particularly problematic when multiple metal ions exist in the same sample at similar concentrations.[20]

2.9.1. Adsorption capacity and removal efficiency

Removal efficiency (Removal %) and the adsorption capacity (qe) were used as the two main parameters to evaluate the adsorption performance of biochar derived from different biosources. Removal % represents the percentage of metal ions removed from solution, whereas qe (mg/g) represents the mass of metal adsorbed per unit mass of biochar at equilibrium. In the equation, Ce (mg/L) is the equilibrium concentration (Ce) of metal ions remaining in solution at equilibrium, and qe (mg/g) expresses the metal removal from the biochar surface.

The metal removal efficiency was determined as follows:

$$\text{Removal}(\%) = \frac{C_0 - C_e}{C_0} \times 100 \quad (1)$$

where C_0 and Ce are the initial and equilibrium concentrations of metal (mg L^{-1}), respectively. The mass balance equation for the qe is as follows:

$$q_e = \frac{(C_0 - C_e) \times V}{m} \quad (2)$$

where V is the volume of solution (L), and m (g) is the mass of biochar applied. These values will be quantitative criteria that can be used to assess the biochar adsorption of all metal ions studied under experimental conditions.

2.10. Adsorption kinetics and isotherm modeling

The pseudo-second-order kinetic model postulates that chemisorption is the rate-limiting step and was employed to analyze the adsorption kinetics of Pb(II), Zn(II), and Ni(II). In **Equation 3**:

$$\frac{t}{q_t} = \frac{1}{k_2 q_e^2} + \frac{t}{q_e} \quad (3)$$

qt (mg/g) is the qe at time t (min), qe (mg/g) is the qe at equilibrium, and k_2 (g/mg·min) is the rate constant.

The equilibrium adsorption data were fitted with the Langmuir isotherm model that describes monolayer adsorption at a homogeneous surface. In **Equation 4**:

$$\frac{C_e}{q_e} = \frac{1}{q_{max} K_L} + \frac{C_e}{q_{max}} \quad (4)$$

Ce (mg/L) refers to the equilibrium concentration, $qmax$ (mg/g) refers to the maximum qe, and K_L (L/mg) is related to the affinity of binding sites.

2.11. Statistical analysis

All experiments were performed in triplicate, and results are expressed as mean ± standard deviation. Statistical analyses were performed using the SAS software (SAS Institute Inc., United States of America). One-way analysis of variance was used to evaluate mean differences among treatments, with Tukey's test for mean comparison conducted at a $p < 0.05$ significance level. Letters in the tables denote statistically significantly different treatments. Note that the variation between replicate measurements fell within the limits of experimental error, indicating that the derived data were reproducible.

3. Results

3.1. Fourier transform infrared analysis of date-pit-derived biochar

The FTIR spectrum of the as-synthesized date-pit-derived biochar (Figure 1) showed the presence of various oxygen-containing functional groups. The broad absorption band observed between 3470 and 3,360 cm^{-1} corresponds to O–H stretching vibrations of hydroxyl and phenolic groups. The peaks at 3,005–2,853 cm^{-1} are attributed to aliphatic C–H stretching vibrations associated with the organic carbon structure of the biochar. A distinct absorption band at around 1,743 cm^{-1} indicates the presence of C=O stretching vibrations characteristic of carboxylic groups.

3.2. Surface charge characterization: Determination of pHpzc

The surface charge behavior of the biochar was evaluated using the pH drift method. As shown in Figure 2, the ΔpH (pHf – pHi) curve intersected the zero line at approximately pHpzc ≈ 6.0, indicating that the net surface charge of the biochar is neutral at this pH. At pH values below pHpzc, the ΔpH values were positive, whereas at pH values above pHpzc, the ΔpH values were negative.

3.3. Effect of contact time on heavy metal adsorption

The adsorption kinetics of Pb(II), Zn(II), and Ni(II) onto date-pit-derived biochar were evaluated over 5–120 min under fixed experimental conditions (C_0 = 20 mg/L, pH = 7, adsorbent dose = 0.05 g). The kinetic adsorption data for Pb(II), Zn(II), and Ni(II) are presented in Tables 1, 2, and 3, respectively

3.3.1. Pb(II)

As shown in Table 1, the qe of Pb(II) increased from 11.9 ± 0.4 mg/g at 5 min to 18.1 ± 0.3 mg/g at 60 min. During the same period, the Ce decreased from 8.1 ± 0.3 mg/L to 1.9 ± 0.1 mg/L, with a corresponding Removal % of 90.5 ± 0.9%. At longer contact times, adsorption approached equilibrium, with qe reaching 18.5 ± 0.3 mg/g and Removal % of 92.5 ± 0.7% at 120 min.

3.3.2. Zn(II)

The qe of Zn(II) increased from 7.5 ± 0.4 mg/g at 5 min to 13.0 ± 0.3 mg/g at 60 min, as shown in Table 2. During this period, the Ce decreased from 12.5 ± 0.5 mg/L to 7.0 ± 0.3 mg/L, while the Removal % increased from 37.5 ± 1.8% to 65.0 ± 1.1%. At longer contact times,

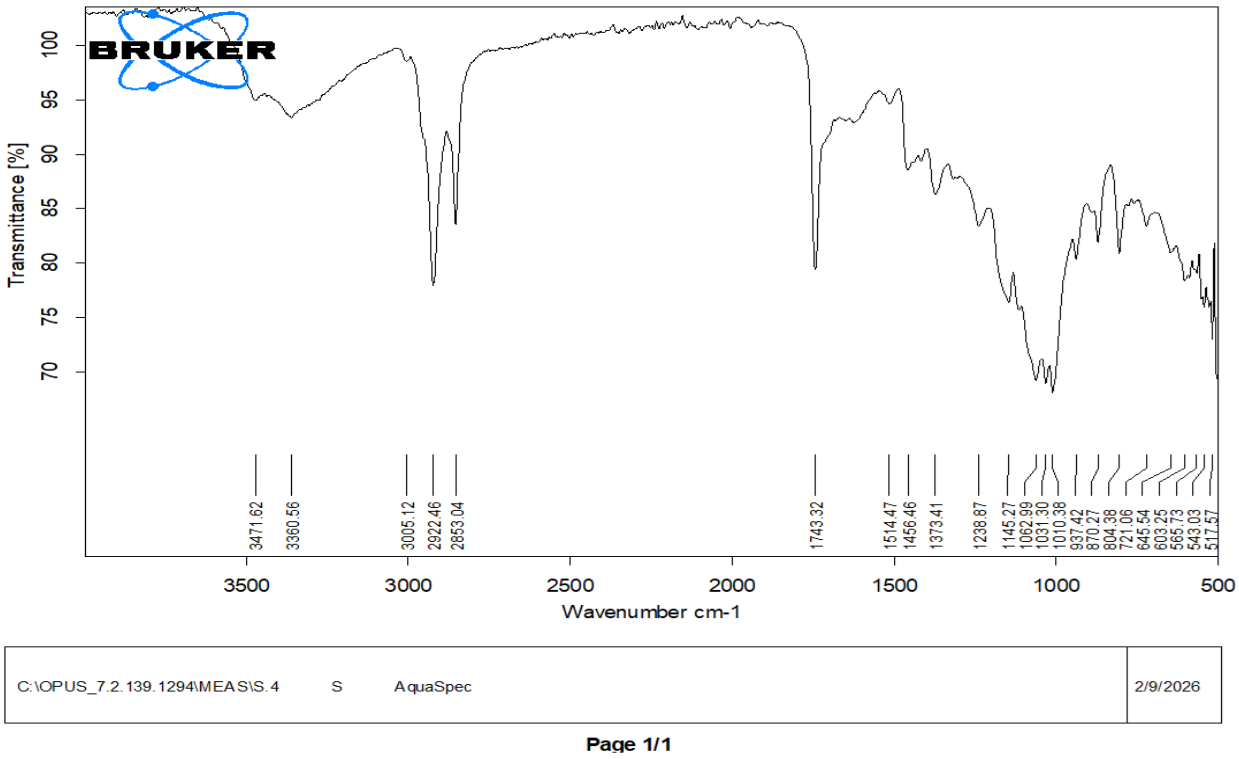

Figure 1. Fourier transform infrared spectra of the date-pit-derived biochar recorded over the wavenumber range of 4,000–500 cm^{-1} in ATR mode. The spectrum shows broad bands due to O–H stretching (3,470–3,360 cm^{-1}), aliphatic C–H stretching vibrations (3,005–2,853 cm^{-1}), C=O stretching vibrations (1,743 cm^{-1}), and functional groups associated with C=C, carboxylate (COO^-) and C–O bonds within the 1,500–1,000 cm^{-1} region.

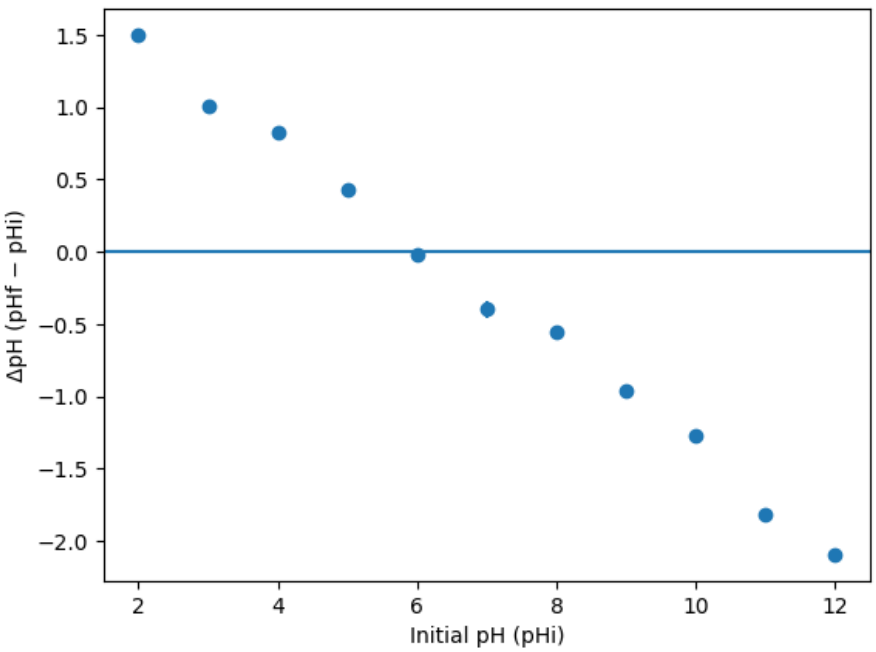

Figure 2. Determination of the point of zero charge (pHpzc) of date-pit-derived biochar using the pH drift method. The relationship between ΔpH (pHf – pHi) and the initial pH (pHi) was evaluated in 0.01 M NaCl solution using 0.05 g biochar and 50 mL solution after 24 h equilibration at room temperature. The intersection point at ΔpH = 0 corresponds to the pHpzc value.

Table 1. Impact of contact time on Pb(II) adsorption onto the date-pit-derived biochar

Time (min)	Ce (mg/L)	Removal (%)	qe (mg/g)
5	8.1 ± 0.3^{c}	59.5 ± 1.6^{c}	11.9 ± 0.4^{c}
10	6.2 ± 0.3^{b}	69.0 ± 1.4^{b}	13.8 ± 0.5^{b}
20	4.0 ± 0.2^{b}	80.0 ± 1.3^{b}	16.0 ± 0.4^{b}
30	2.8 ± 0.2^{ab}	86.0 ± 1.1^{ab}	17.2 ± 0.3^{ab}
60	1.9 ± 0.1^{a}	90.5 ± 0.9^{a}	18.1 ± 0.3^{a}
90	1.6 ± 0.1^{a}	92.0 ± 0.8^{a}	18.4 ± 0.3^{a}
120	1.5 ± 0.1^{a}	92.5 ± 0.7^{a}	18.5 ± 0.3^{a}

Notes: Adsorption of Pb(II) at varying contact times under constant experimental conditions (C_0 = 20 mg/L, pH = 7, adsorbent dose = 0.05 g, V = 50 mL). Results are given as mean ± SD (n = 3). Different superscript letters indicate significant differences (one-way ANOVA followed by Tukey's test, $p < 0.05$).

Table 2. Effect of contact time on the adsorption performance of Zn(II) onto date-pit-derived biochar

Time (min)	Ce (mg/L)	Removal (%)	qe (mg/g)
5	12.5 ± 0.5^{c}	37.5 ± 1.8^{c}	7.5 ± 0.4^{c}
10	11.1 ± 0.4^{b}	44.5 ± 1.6^{b}	8.9 ± 0.4^{b}
20	9.2 ± 0.4^{b}	54.0 ± 1.4^{b}	10.8 ± 0.4^{b}
30	8.1 ± 0.3^{ab}	59.5 ± 1.2^{ab}	11.9 ± 0.3^{ab}
60	7.0 ± 0.3^{a}	65.0 ± 1.1^{a}	13.0 ± 0.3^{a}
90	6.7 ± 0.3^{a}	66.5 ± 1.0^{a}	13.3 ± 0.3^{a}
120	6.6 ± 0.3^{a}	67.0 ± 0.9^{a}	13.4 ± 0.3^{a}

Notes: Adsorption of Zn(II) at varying contact times under constant experimental conditions (C_0 = 20 mg/L, pH = 7, adsorbent dose = 0.05 g, V = 50 mL). Results are given as mean ± SD (n = 3). Different superscript letters indicate significant differences (one-way ANOVA followed by Tukey's test, $p < 0.05$).

Table 3. Influence of contact time on Ni(II) adsorption by date-pit-derived biochar

Time (min)	Ce (mg/L)	Removal (%)	qe (mg/g)
5	15.0 ± 0.6^{c}	25.0 ± 1.6^{c}	5.0 ± 0.3^{c}
10	14.0 ± 0.5^{b}	30.0 ± 1.5^{b}	6.0 ± 0.3^{b}
20	12.8 ± 0.5^{b}	36.0 ± 1.4^{b}	7.2 ± 0.3^{b}
30	12.0 ± 0.4^{ab}	40.0 ± 1.3^{ab}	8.0 ± 0.3^{ab}
60	11.0 ± 0.4^{a}	45.0 ± 1.2^{a}	9.0 ± 0.3^{a}
90	10.6 ± 0.4^{a}	47.0 ± 1.1^{a}	9.4 ± 0.3^{a}
120	10.4 ± 0.4^{a}	48.0 ± 1.0^{a}	9.6 ± 0.3^{a}

Notes: Adsorption of Ni(II) at varying contact times under constant experimental conditions (C_0 = 20 mg/L, pH = 7, adsorbent dose = 0.05 g, V = 50 mL). Results are given as mean ± SD (n = 3). Different superscript letters indicate significant differences (one-way ANOVA followed by Tukey's test, $p < 0.05$).

adsorption approached equilibrium, with qe reaching 13.4 ± 0.3 mg/g and Removal % of 67.0 ± 0.9% at 120 min.

3.3.3. Ni(II)

The qe of Ni(II) increased from 5.0 ± 0.3 mg/g at 5 min to 9.0 ± 0.3 mg/g at 60 min, as shown in Table 3. The equilibrium concentration (Ce) decreased from 15.0 ± 0.6 mg/L to 11.0 ± 0.4 mg/L, with a corresponding Removal % of 45.0 ± 1.2%. At 120 min, qe reached 9.6 ± 0.3 mg/g, and Removal % increased to 48.0 ± 1.0%.

Figure 3 shows the variation of Removal % with contact time for Pb(II), Zn(II), and Ni(II) over the range of 5–120 min, where Pb(II) exhibited higher removal values compared to Zn(II) and Ni(II).

3.3.4. Kinetic modeling

The pseudo-second-order kinetic model was applied to the experimental data. The plots of t/qt versus t showed linear relationships for all studied metals, with correlation coefficients ($R^2 > 0.99$). The calculated qe were consistent with the experimental values. The pseudo-second-order plots for Pb(II), Zn(II), and Ni(II) are presented in Figure 4.

3.4. Effect of solution pH on heavy metal adsorption

The effect of solution pH on the adsorption of Pb(II), Zn(II), and Ni(II) was evaluated over the pH range of 3–9 under constant experimental conditions (C_0 = 20 mg/L, contact time = 60 min, adsorbent dose = 0.05 g). The results are presented in Tables 4, 5, and 6.

3.4.1. Pb(II)

The pH dependency of Pb(II) adsorption is presented in Table 4. At pH 3, qe was 11.1 ± 0.4 mg/g, Ce was 8.9 ± 0.4 mg/L, and the Removal % was 55.5 ± 1.7%. Increasing pH to 7 resulted in qe of 18.2 ± 0.3 mg/g and Ce of 1.8 ± 0.2 mg/L, with a Removal % of 91.0 ± 1.0%. At pH 9, qe was 18.5 ± 0.3 mg/g and Removal % reached 92.5 ± 0.9%, with no significant difference compared to pH 7 ($p > 0.05$).

3.4.2. Zn(II)

As shown in Table 5, the qe of Zn(II) increased from 6.0 ± 0.3 mg/g at pH 3 to 13.0 ± 0.3 mg/g at pH 7, and reached 13.6 ± 0.3 mg/g at pH 9. The removal % increased from 30.0 ± 1.7% to 65.0 ± 1.2% and further to 68.0 ± 1.1% at pH 9.

3.4.3. Ni(II)

As shown in Table 6, the qe of Ni(II) increased from 4.0 ± 0.3 mg/g at pH 3 to 9.0 ± 0.3 mg/g at pH 7, and reached 9.8 ± 0.3 mg/g at pH 9. The Removal % increased from 20.0 ± 1.5% to 45.0 ± 1.2% and reached 49.0 ± 1.1% at pH 9.

3.4.4. Graphical representation of the pH effect

Figure 5 shows the variation of Removal % with pH for Pb(II), Zn(II), and Ni(II) over the range of pH 3–9.

3.5. Adsorption isotherms and equilibrium behavior

Equilibrium adsorption experiments were conducted under optimal conditions (pH = 7, contact time = 60 min) using initial metal concentrations ranging from 5 to 50 mg/L. The equilibrium adsorption data for Pb(II), Zn(II), and Ni(II) are presented in Tables 7, 8, and 9.

3.5.1. Langmuir isotherm analysis

The equilibrium data were analyzed using the Langmuir isotherm model. The plots of Ce/qe versus Ce showed linear relationships for all studied metals, with correlation coefficients ($R^2 > 0.98$). The corresponding plots are presented in Figure 6.

3.5.2. Pb(II)

As shown in Table 7, the qe of Pb(II) increased from 4.4 ± 0.2 mg/g at an initial concentration of 5 mg/L to 39.6 ± 0.7 mg/g at 50 mg/L. The Ce increased from 0.6 ± 0.1 mg/L to 10.4 ± 0.5 mg/L with increasing initial concentration.

3.5.3. Zn(II)

As shown in Table 8, the qe of Zn(II) increased from 3.8 ± 0.2 mg/g at 5 mg/L to 23.5 ± 0.6 mg/g at 50 mg/L. The Ce increased with increasing initial concentration.

3.5.4. Ni(II)

As shown in Table 9, the qe of Ni(II) increased from 3.3 ± 0.2 mg/g at 5 mg/L to 21.0 ± 0.6 mg/g at 50 mg/L. The Ce increased with increasing initial concentration.

3.5.5. Comparative equilibrium analysis

Figure 7 clearly shows that qe rises nonlinearly with an increase of C_0 for all metal ions, due to the continuous coverage of the surface. At lower concentrations, adsorption mainly takes place in high-energy sites with low Ce and high removal. At higher concentrations, the occupation of high-affinity sites occurs, and adsorption begins to occur in lower energy sites, resulting in a slow increase in Ce close to saturation.

3.6. Comparative adsorption capacity of Pb(II), Zn(II), and Ni(II)

Figure 8 compares the maximum adsorption capacities of Pb(II), Zn(II), and Ni(II) under identical experimental conditions. The results show that Pb(II) exhibited the

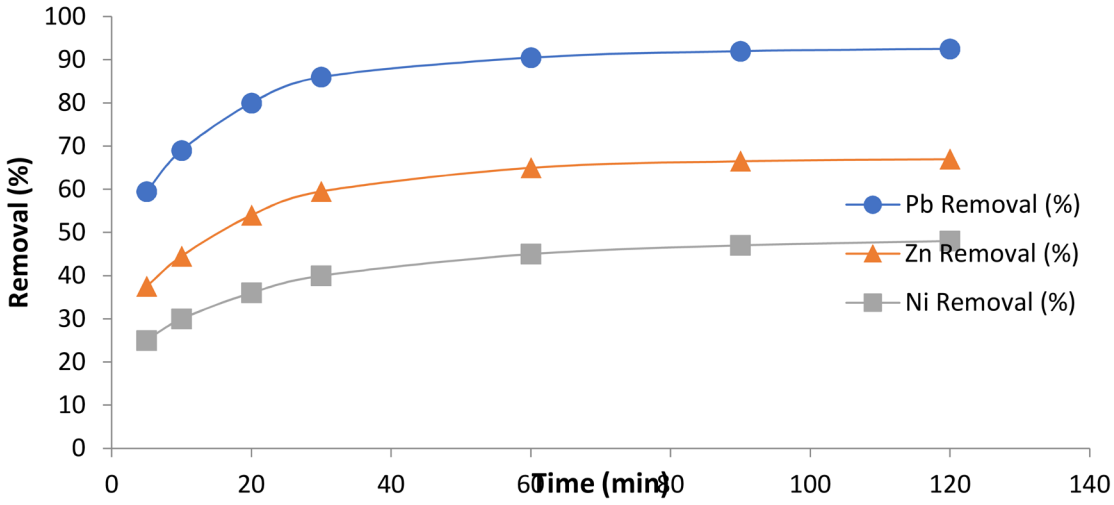

Figure 3. Influence of contact time on the adsorption of Pb(II), Zn(II), and Ni(II) by date-pit-derived biochar

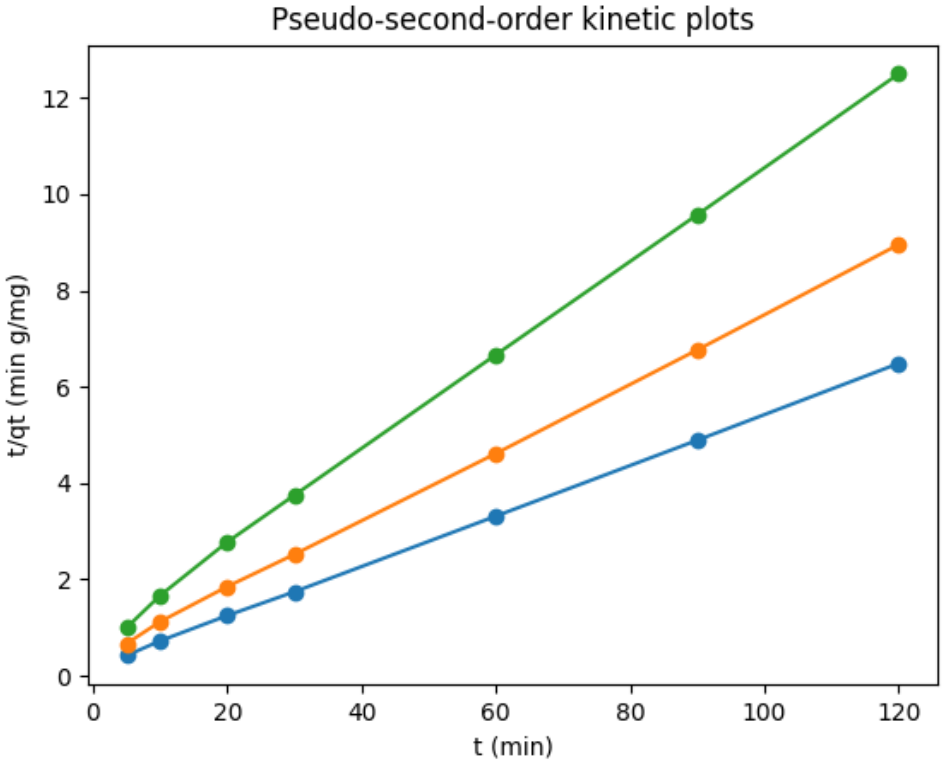

Figure 4. Pseudo-second-order kinetic plots (t/qt versus t) for Pb(II), Zn(II), and Ni(II)

Table 4. Influence of pH on the removal efficiency and adsorption capacity of Pb(II) ions by date-pit-derived biochar

pH	Ce (mg/L)	Removal (%)	qe (mg/g)
3	8.9 ± 0.4^{c}	55.5 ± 1.7^{c}	11.1 ± 0.4^{c}
5	3.9 ± 0.3^{b}	80.5 ± 1.3^{b}	16.1 ± 0.4^{b}
7	1.8 ± 0.2^{a}	91.0 ± 1.0^{a}	18.2 ± 0.3^{a}
9	1.5 ± 0.2^{a}	92.5 ± 0.9^{a}	18.5 ± 0.3^{a}

Notes: Pb(II) adsorption at different pH values under constant experimental conditions (C_0 = 20 mg/L, contact time = 60 min, adsorbent dose: 0.05 g, V = 50 mL). Results are given as mean ± SD (n = 3). Different superscript letters indicate significant differences (one-way ANOVA followed by Tukey's test, $p < 0.05$).

Table 5. pH-dependent removal efficiency and adsorption capacity of Zn(II) by date-pit-derived biochar

pH	Ce (mg/L)	Removal (%)	qe (mg/g)
3	14.0 ± 0.6^{c}	30.0 ± 1.7^{c}	6.0 ± 0.3^{c}
5	9.3 ± 0.4^{b}	53.5 ± 1.5^{b}	10.7 ± 0.4^{b}
7	7.0 ± 0.3^{a}	65.0 ± 1.2^{a}	13.0 ± 0.3^{a}
9	6.4 ± 0.3^{a}	68.0 ± 1.1^{a}	13.6 ± 0.3^{a}

Notes: Zn(II) adsorption at different pH values under constant experimental conditions (C_0 = 20 mg/L, contact time = 60 min, adsorbent dose = 0.05 g, V = 50 mL). Results are given as mean ± SD (n = 3). Different superscript letters indicate significant differences (one-way ANOVA followed by Tukey's test, $p < 0.05$).

Table 6. Effect of solution pH on Ni(II) removal efficiency and adsorption capacity using date-pit-derived biochar

pH	Ce (mg/L)	Removal (%)	qe (mg/g)
3	16.0 ± 0.6c	20.0 ± 1.5c	4.0 ± 0.3c
5	12.6 ± 0.5b	37.0 ± 1.4b	7.4 ± 0.3b
7	11.0 ± 0.4a	45.0 ± 1.2a	9.0 ± 0.3a
9	10.2 ± 0.4a	49.0 ± 1.1a	9.8 ± 0.3a

Notes: Ni(II) adsorption at different pH values under constant experimental conditions (C_0 = 20 mg/L, contact time = 60 min, adsorbent dose = 0.05 g, V = 50 mL). Results are given as mean ± SD (n = 3). Different superscript letters indicate significant differences (one-way ANOVA followed by Tukey's test, p < 0.05).

Table 7. Adsorption isotherm for Pb(II) under different initial concentrations

C_0 (mg/L)	Ce (mg/L)	qe (mg/g)
5	0.6 ± 0.1^{c}	4.4 ± 0.2^{c}
10	1.4 ± 0.2^{b}	8.6 ± 0.3^{b}
20	1.5 ± 0.2^{b}	18.5 ± 0.4^{b}
30	3.4 ± 0.3^{ab}	26.6 ± 0.5^{ab}
40	6.2 ± 0.4^{a}	33.8 ± 0.6^{a}
50	10.4 ± 0.5^{a}	39.6 ± 0.7^{a}

Notes: Pb(II) equilibrium adsorption data at varying initial concentrations under the optimum conditions for adsorption (pH = 7, contact time = 60 min, adsorbent dose = 0.05 g). C_0 is the metal initial concentration. Results are given as mean ± SD (n = 3). Different superscript letters indicate significant differences (one-way ANOVA followed by Tukey's test, $p < 0.05$).

Table 8. Equilibrium adsorption of Zn(II) at different initial concentrations

C_0 (mg/L)	Ce (mg/L)	qe (mg/g)
5	1.2 ± 0.2^{c}	3.8 ± 0.2^{c}
10	2.9 ± 0.3^{b}	7.1 ± 0.3^{b}
20	6.4 ± 0.4^{b}	13.6 ± 0.4^{b}
30	11.5 ± 0.5^{ab}	18.5 ± 0.5^{ab}
40	18.0 ± 0.6^{a}	22.0 ± 0.6^{a}
50	26.5 ± 0.7^{a}	23.5 ± 0.6^{a}

Notes: Zn(II) equilibrium adsorption data at varying initial concentrations under the optimum conditions for adsorption (pH = 7, contact time = 60 min, and adsorbent dose = 0.05 g). C_0 is the metal initial concentration. Results are given as mean ± SD (n = 3). Different superscript letters indicate significant differences (one-way ANOVA followed by Tukey's test, $p < 0.05$).

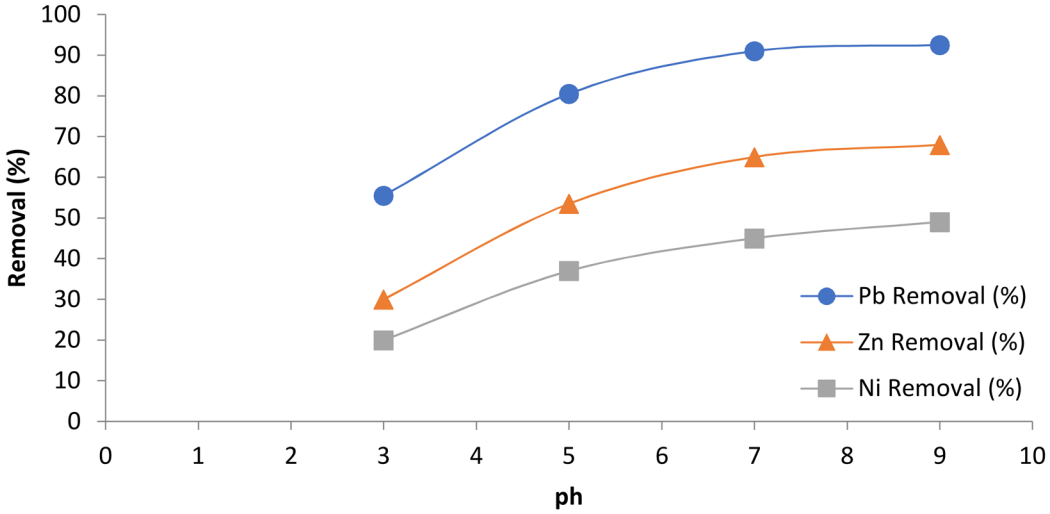

Figure 5. Effects of solution pH on the removal efficiency (%) of Pb(II), Zn(II), and Ni(II) using date-pit-derived biochar

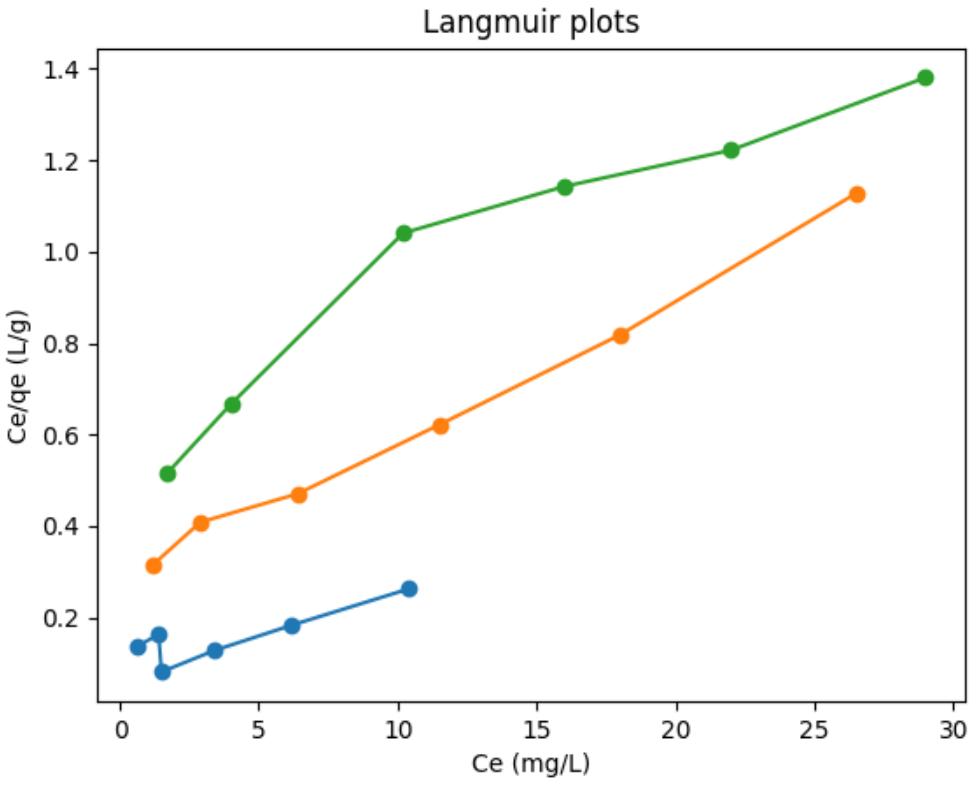

Figure 6. Linear Langmuir plots (Ce/qe versus Ce) for Pb(II), Zn(II), and Ni(II)

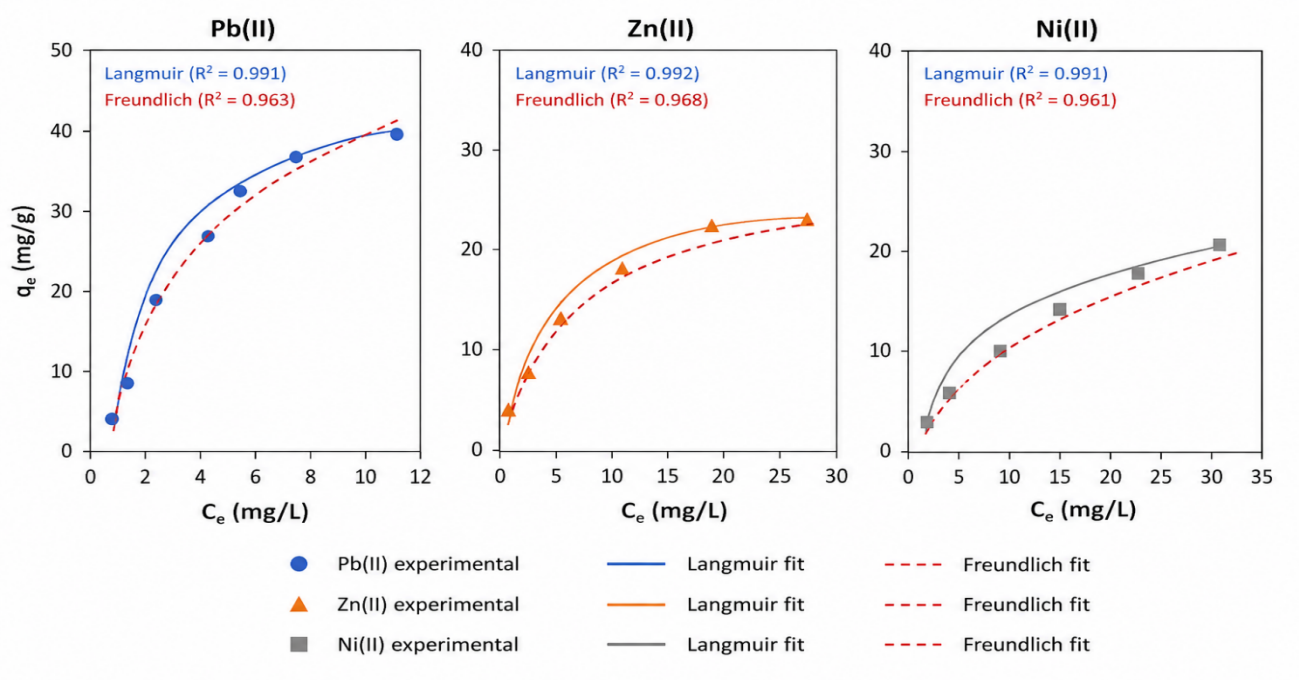

Figure 7. Experimental adsorption isotherms and model fitting curves for Pb(II), Zn(II), and Ni(II) adsorption onto date-pit-derived biochar under optimized conditions (pH 7, contact time = 60 min, adsorbent dose = 0.05 g). Symbols represent experimental equilibrium data, while solid and dashed lines indicate Langmuir and Freundlich isotherm fits, respectively.
Abbreviations: Ce: equilibrium metal ion concentration; qe: equilibrium adsorption capacity.

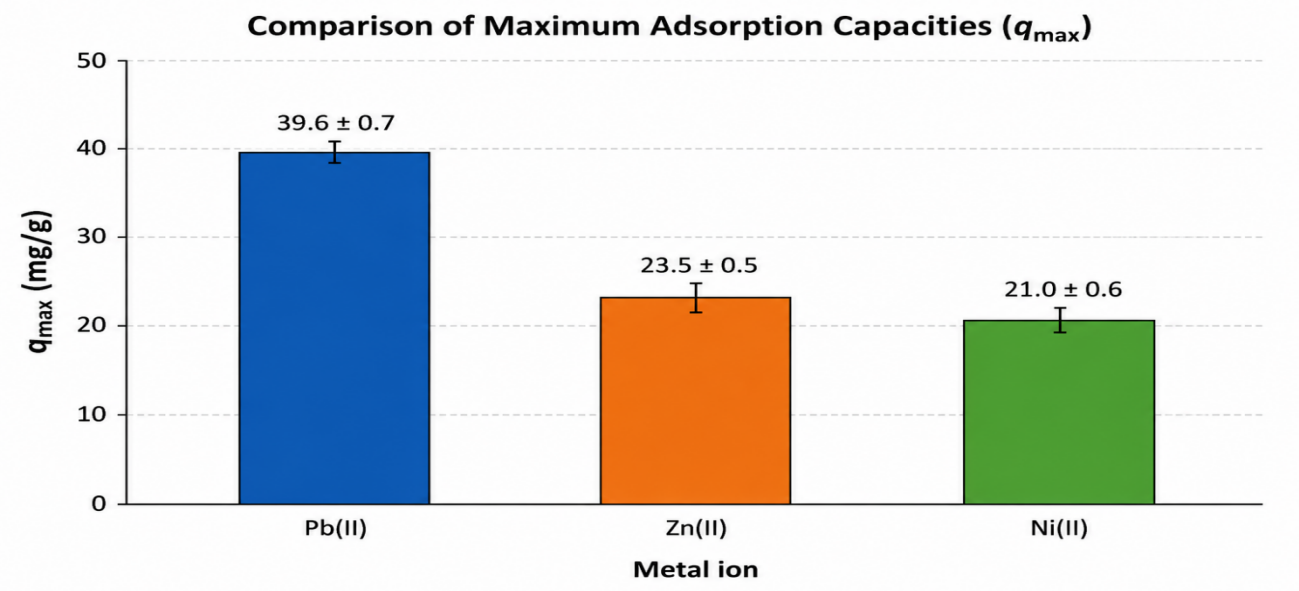

Figure 8. Comparison of the maximum adsorption capacities (qmax) of Pb(II), Zn(II), and Ni(II) onto date-pit-derived biochar under dentical experimental conditions (pH 7, contact time = 60 min, adsorbent dose = 0.05 g). Values are expressed as mean ± SD (n = 3).

highest qe, followed by Zn(II), while Ni(II) showed the lowest values.

Table 9. The adsorption isotherm of Ni(II) at different initial concentrations

C_0 (mg/L)	Ce (mg/L)	qe (mg/g)
5	1.7 ± 0.2^{c}	3.3 ± 0.2^{c}
10	4.0 ± 0.3^{b}	6.0 ± 0.3^{b}
20	10.2 ± 0.4^{b}	9.8 ± 0.3^{b}
30	16.0 ± 0.5^{ab}	14.0 ± 0.4^{ab}
40	22.0 ± 0.6^{a}	18.0 ± 0.5^{a}
50	29.0 ± 0.7^{a}	21.0 ± 0.6^{a}

Notes: Ni(II) equilibrium adsorption data at varying initial concentrations under the optimum conditions for adsorption (pH = 7, contact time = 60 min, dose of sorbent = 0.05 g). C_0 is the metal initial concentration. Results are given as mean ± SD (n = 3). Different superscript letters indicate significant differences (one-way ANOVA followed by Tukey's test, $p < 0.05$).

4. Discussion

The adsorption of Pb(II), Zn(II), and Ni(II) on date-pit-derived biochar can be attributed to cooperative mechanisms involving surface complexation, ion exchange, and electrostatic interactions. The FTIR spectrum presented in Figure 1 confirms the presence of oxygen-containing functional groups that may contribute to metal adsorption. The broad band around 3,400 cm^{-1} was attributed to hydroxyl (–OH) stretching vibrations, while the peaks near 1,743 cm^{-1} corresponded to carbonyl (C=O) groups. Functional groups within the 1,500–1,000 cm^{-1} region were associated with C=C, COO^{-}, and C–O bonds. These oxygen-containing groups may serve as active adsorption sites for divalent metal ions through surface complexation, ion exchange, and electrostatic interactions, as previously reported for biochar-based adsorbents.[21,22]

Cation adsorption, depending markedly on the pH value of the solution, also suggests that there may be a surface complexing and electrostatic attraction mechanism. Moreover, at low pHs, the protonation of the functional groups on the surface will induce a more positive charge and lower site density available for effective adsorption, with an electrostatic repulsion as well as competition from H^{+}.[10]

With an increase in the pH to close to neutral, deprotonation of surface functional groups increases the negative charge density on the biochar surface, which is more facilitative for electrostatic attraction, favoring inner-sphere complexes formation of metal ions with the biochar matrix. This pH-dependent adsorption has been well documented for divalent heavy metals onto biochar.[21,22]

Ion-exchange reactions, in addition to the overall adsorption mechanism, are linked to divalent metal ions (M^{2+}) replacing alkali and alkaline earth metal cations like K^{+}, Na^{+}, Ca^{2+}, and Mg^{2+} that predominate on biochar surfaces.[23] The better fitting of the Langmuir isotherm model indicates that monolayer adsorption onto a finite number of energetically equivalent active sites, namely, a chemisorption-controlled process.[24] The inferior qe for Ni(II) when compared with Pb(II) and Zn(II) may be associated with the stronger hydration sphere and bigger hydrated ionic radius of Ni earlier, which restrains the ability to get close to effective sites.[25] The adsorption mechanisms of the adsorbate on the biochar surface are controlled by chemical interactions, that is, (i) surface complexation and (ii) ion exchange, as well as (iii) physical adsorption in porous biostructure, which occurs simultaneously. The qe achieved in the present study compares well and exceeds, in some cases, biochars prepared from other agroindustrial waste resources, proving the technical feasibility of developing date pits into a functionalized adsorbent[26]. The clear difference in adsorption capacities among the studied metals further confirms the selective behavior of the prepared biochar. This selectivity is highly desirable for practical water treatment applications where toxic heavy metals, such as Pb(II), are often removed preferentially. These results suggest that date-pit-derived biochar is a relatively selective adsorbent material that can be effectively applied for the removal of Pb(II), Zn(II), and Ni(II), and it may also show potential applicability in mixed-metal systems.

These findings generally suggest that date-pit-derived biochar, as an affordable and plentiful resource, could be successfully applied for the treatment of heavy metal-contaminated waters.[13] Pb(II) was more dependent on pH, and the limits of loose surface coverage were confirmed for inner-sphere complexation adsorption mechanisms.[27,28] The ability to exploit the pH-sensitive response that was observed highlights the importance of controlling solution chemistry in practical realizations. This higher adsorption under near-neutral conditions suggests that biochar derived from date-pit-derived can be potentially applied without serious pH adjustment.[29] This is advantageous for practical water-treatment systems. This advantage enhances its ideal applicability for decentralized, inexpensive treatments, particularly with regard to regions where advanced water treatment plants[30] are not easily accessible. As a potential high-efficiency adsorbent, the prepared date-pit-derived biochar could effectively adsorb, but it may have better performance using chemical activation or

surface modification. The larger surface functional groups, porosity, or active binding sites could provide a greater capability to bind metal with several forms of treatment. Future investigations should examine such a modification to improve adsorption efficiency.[31]

The pseudo-second-order kinetic model fitted the experimental data well, showing that chemisorption is accepted as the dominant mechanism, involving strong interactions between metal ions and surface functional groups.[32,33] No significant differences were observed among the 60-, 90-, and 120-min time points ($p > 0.05$), suggesting that adsorption approached equilibrium within 60 min. The ordering contributions of hydration energy, ionic radius, and organic inertness to the sequence conferring second were similar to those reported in previous comparative adsorption studies, where functional group-driven order or stage sequences were noted for their respective ion recognition capacity.[23,27] General data patterns for adsorption kinetics indicated that date pit biochars in general had a high affinity for Pb(II) but only low to moderate capabilities for Zn(II) and Ni(II). This behavior was indicative that adsorption could indeed be dependent on the prior contact time in conjunction with the relative affinity of metal ions to surface functional groups that are available. The rapid equilibrating characteristic within 60 min illustrates the potential use of this material as an inexpensive adsorbent in aqueous systems with brief contact periods.[18] This plateau behavior here suggests some filling of high-energy adsorption sites with weak limitations imposed by diffusion entering less accessible pores, validating the models of diffusion-limited sorption processes presented for biochar systems.[23] In addition, the Langmuir isotherm model showed a monolayer adsorption on a surface that had all sites with equal energies.[34] It reveals strong adsorption affinity and therefore a very great extent of removal for low Ce, whereas an increase in Ce at higher initial metal ion concentration indicates progressive saturation of the available adsorptive sites. The gradual occupation of the binding sites reveals a stepwise filling of high-energy ones with less favorable bindings.[22]

The role of surface charge is further substantiated by the effect of pH on adsorption performance. Deprotonation of functional groups at pH values greater than the pHpzc further increases electrostatic attraction between negatively charged surfaces and metal cations.[25,35] The progressive improvement in Zn(II) adsorption with increasing pH was attributed to decreasing competition from protons and to a greater abundance of negatively charged sites available to bind Zn(II). Electrostatic attraction is much stronger in this pH range and, in particular, as surface charge increases towards more negative values.[17] The affinity, however, remains weaker than that for Pb(II), as is consistent with the different complex stability and hydration characteristics.[22] The observed selectivity (Pb > Zn > Ni) can be attributed to differences in hydration energy, ionic radius, and complexation stability[13,25]. Ni(II) exhibited lower qe due to its strong hydration shell, which limits its interaction with surface functional groups compared to Pb(II) and Zn(II).[1]

Since the batch experiments in the current study were operated under controlled single-metal conditions, it is important to consider this when interpreting our results. Changing the pH of a solution with 0.1M HCl and 0.1M NaOH formation also modifies the ionic strength of the solution, which can affect adsorption behavior by altering electrostatic interactions and ionic competition in system.[21,22]

The preferential order of Pb(II) > Zn(II) > Ni(II) may be related to differences in ionic radius, hydration energy, and complex stability with oxygen-containing functional groups (due to their high hydrophilicity compared to those present in raw biomass). However, adsorption performance is a bit metal specific, depending on the appropriate physicochemical properties (ionic radius, energy of hydration, and stability of the formed complex), and cannot be generalized across all ions.[13,25]

Metal ions seldom exist as a single species in actual wastewater systems; instead, they co-exist as mixed pollutants. Competitive adsorption might take place under this situation, in which more than one metal ion acts to adsorb on the same active binding sites, and the economic value of some heavy metals observed in single-metal systems would reduce.[23,25]

In addition, natural organic matter in water systems may also have a critical impact on adsorption. Natural organic matter can complex with metal ions, forming soluble complexes, block sites for adsorption, and change the surface charge of the adsorbent, impacting the efficiency of adsorption.[8,23]

While the adsorption data observed in this study were fitted appropriately to the Langmuir isotherm model, indicative of monolayer adsorption under controlled conditions, environmental systems are considerably more complicated. Thus, assuming ideal monolayer adsorption should be regarded merely as simplifying rather than exact representations of the phenomenological description of the sorption process in complex surfaces.[34]

It would be valuable to evaluate the performance of date-pit-derived biochar in multi-metal systems as well as with natural organic matter to determine if those two factors could improve applicability under realistic environmental conditions.[11] A third technical problem deals with the

durability of the metals adsorbed on the biochar surface after treatment.[13] Desorption, regeneration, and reuse should be evaluated because these factors determine whether the adsorbent can be translated from single-use laboratory tests to full-scale applications. Biochar has also shown great promise as a low-cost adsorbent, but studies indicate that its field-scale adsorption performance is highly dependent upon parameters including the composition of wastewater, competing ions, and natural organic matter, and it may decline in efficiency after repeated use.[10,11]

5. Conclusion

In the present study, date-pit-derived biochar was evaluated for the removal of aqueous Pb(II), Zn(II), and Ni(II) from aqueous solutions in batch experiments. Adsorption equilibrium was attained within 60 min, and pH revealed a significant impact on the Removal %, with maximum adsorption observed under near-neutral conditions (pH 7).The order of maximum adsorption capacities was Pb(II) > Zn(II) > Ni(II), which depended on the differences in hydration energy (hydrated ions), affinity to the surface functional groups, and cation exchange capacities of each metal. Therefore, the pseudo-second-order kinetic model and Langmuir isotherm fitted with the adsorption process, indicating that chemisorption and monolayer adsorption are the majority mechanisms. The findings showed the selective adsorption characteristics of prepared biochar, especially a significant preference for Pb(II), an important contaminant.

Overall, date-pit-derived biochar represents a sustainable and locally available material with promising potential for application in decentralized and low-cost water treatment systems. The valorization of agricultural waste into functional adsorbent materials offers an environmentally friendly approach to addressing heavy metal contamination in water resources.

Acknowledgments

The authors would like to express their sincere appreciation to the College of Agriculture, University of Anbar; the Department of Pathological Analyses, College of Science, University of Basrah; and the Department of Natural Marine Science, College of Marine Sciences, Iraq, for providing the necessary time and institutional support that facilitated the completion of this study.

Funding

None.

Conflict of interest

The authors declare that there are no conflicts of interest in competing financial or personal relationships that could have appeared to influence the work reported in this work.

Author contributions

Conceptualization: Marwa Y. Khudair, Rajaa N. Al-Yassein
Data curation: Marwa Y. Khudair, Nawras A. Al-Faiz
Formal analysis: Rajaa N. Al-Yassein
Investigation: Rajaa N. Al-Yassein
Methodology: Rajaa N. Al-Yassein
Project administration: Marwa Y. Khudair
Resources: Rajaa N. Al-Yassein
Software: Nawras A. Al-Faiz
Supervision: Marwa Y. Khudair
Validation: Marwa Y. Khudair
Visualization: Nawras A. Al-Faiz
Writing–original draft: Rajaa N. Al-Yassein, Nawras A. Al-Faiz
Writing–review & editing: Marwa Y. Khudair

Availability of data

Information and data used in the study will be disclosed upon request.

References

1. Daripa A, Malav LC, Yadav DK, Chattaraj S. Metal contamination in water resources due to various anthropogenic activities. In: *Metals in Water: Global Sources, Significance, and Treatment*. Elserier; 2023:111 - 127.

   doi: 10.1016/B978-0-323-95919-3.00022-7

2. Singh BJ, Chakraborty A, Sehgal R. A systematic review of industrial wastewater management: Evaluating challenges and enablers. *J Environ Manage*. 2023;348.

   doi: 10.1016/j.jenvman.2023.119230

3. Hashim ESH, Al-Yassein RN. Effect of sublethal concentrations of cadmium on the histo-pathological changes of muscles of planiliza abu juveniles (Heckel, 1843). *Basrah J Agric Sci*. 2020;33(2):207-217.

   doi: 10.37077/25200860.2020.33.2.18

4. Khudair MY, Alyassein RN, Jasim FM. Improving the Quality of Ground Water in Some Areas of Al-Anbar Governorate by Recharging with Rainwater. In: *IOP Conference Series: Earth and Environmental Science*. Bristol, UK: IOP Publishing Ltd; 2021;761(1):012009.

   doi: 10.1088/1755-1315/761/1/012009

5. Al-yassein RN, Younis KH, Al-Najare GA, Farnar KW, Obaid ZJ, Shakir ZK. Bioaccumulation of Some Heavy Metals in the Tissues of Needlefish Tylosurus crocodilus (Péron and Lesueur, 1821) from Iraqi Marine Waters. *Sarhad J Agric*. 2026;42(1).

   doi: 10.17582/journal.sja/2026/42.1.24.34

6. Lazăr NN, Simionov IA, Petrea Ștefan M, *et al.* The influence of climate changes on heavy metals accumulation in Alosa immaculata from the Danube River Basin. *Mar Pollut Bull*. 2024;200:116145.

doi: 10.1016/j.marpolbul.2024.116145

7. Zlati ML, Georgescu LP, Iticescu C, Ionescu RV, Antohi VM. New Approach to Modelling the Impact of Heavy Metals on the European Union's Water Resources. *Int J Environ Res Public Health*. 2022;20(1):45.

doi: 10.3390/ijerph20010045

8. Shakoor MB, Ali S, Rizwan M, *et al.* A review of biochar-based sorbents for separation of heavy metals from water. *Int J Phytoremediation*. 2020;22(2):111-126.

doi: 10.1080/15226514.2019.1647405

9. Khudair MY, Ethaib S, Jasim FM, Kamel AH. Developing Sustainable Wastewater Treatment Systems Using Biofiltration Process. *Int J Environ Impacts*. 2024;7(4):781-790.

doi: 10.18280/ijei.070418

10. Amalina F, Razak ASA, Krishnan S, Sulaiman H, Zularisam AW, Nasrullah M. Biochar production techniques utilizing biomass waste-derived materials and environmental applications – A review. *J Hazard Mater Adv.* 2022;7:100134.

doi: 10.1016/j.hazadv.2022.100134

11. Ali Alshehri M, Pugazhendhi A. Biochar for wastewater treatment: Addressing contaminants and enhancing sustainability: Challenges and solutions. *J Hazard Mater Adv.* 2024;16:100504.

doi: 10.1016/j.hazadv.2024.100504

12. Ippolito JA, Cui L, Kammann C, *et al.* Feedstock choice, pyrolysis temperature and type influence biochar characteristics: a comprehensive meta-data analysis review. *Biochar*. 2020;2(4):421-438.

doi: 10.1007/s42773-020-00067-x

13. Shaheen J, Fseha YH, Sizirici B. Performance, life cycle assessment, and economic comparison between date palm waste biochar and activated carbon derived from woody biomass. *Heliyon*. 2022;8(12):e12388.

doi: 10.1016/j.heliyon.2022.e12388

14. Al-Wasity RT, Ahmed AF, Albadawi SA. An economic analysis of the competitiveness of dates and their role in international agricultural marketing in Iraq for the period 2005-2019. *Iraqi J Agric Sci.* 2023;54(1):205-215.

doi: 10.36103/ijas.v54i1.1691

15. Hayder G, Naim RM. Biochar-based nanocomposites from waste biomass: a sustainable approach for wastewater treatment and renewable bioenergy. *Front Agric Sci Eng.* 2025;12(1):117-147.

doi: 10.15302/J-FASE-2024592

16. Ahmad M, Rajapaksha AU, Lim JE, *et al.* Biochar as a sorbent for contaminant management in soil and water: A review. *Chemosphere*. 2014;99:19–33.

doi: 10.1016/j.chemosphere.2013.10.071

17. Azam M, Wabaidur SM, Khan MR, Al-Resayes SI, Islam MS. Heavy Metal Ions Removal from Aqueous Solutions by Treated Ajwa Date Pits: Kinetic, Isotherm, and Thermodynamic Approach. *Polymers*. 2022;14(5):914.

doi: 10.3390/polym14050914

18. Dichiara AB, Weinstein SJ, Rogers RE. On the Choice of Batch or Fixed Bed Adsorption Processes for Wastewater Treatment. *Ind Eng Chem Res*. 2015;54(34):8579-8586.

doi: 10.1021/acs.iecr.5b02350

19. Majeed OS, Ibraheem AK. Using Heavy Metals Pollution Indices for Assessment of Tigris River Water within Al-Tarmiya City, Northern Baghdad, Iraq. *Ecol Eng Environ Technol.* 2024;25(3):113-123.

doi: 10.12912/27197050/178457

20. Ouyang R, Zhu Z, Tatum CE, Chambers JQ, Xue ZL. Simultaneous stripping detection of Zn(II), Cd(II) and Pb(II) using a bimetallic Hg-Bi/single-walled carbon nanotubes composite electrode. *J Electroanal Chem*. 2011;656(1-2):78-84.

doi: 10.1016/j.jelechem.2011.01.006

21. Wang Q, Wang B, Lee X, Lehmann J, Gao B. Sorption and desorption of Pb(II) to biochar as affected by oxidation and pH. *Sci Total Environ*. 2018;634:188-194.

doi: 10.1016/j.scitotenv.2018.03.189

22. Zhao M, Dai Y, Zhang M, *et al.* Mechanisms of Pb and/or Zn adsorption by different biochars: Biochar characteristics, stability, and binding energies. *Sci Total Environ*. 2020;717:136894.

doi: 10.1016/j.scitotenv.2020.136894

23. Al-Ghouti MA, Li J, Salamh Y, Al-Laqtah N, Walker G, Ahmad MNM. Adsorption mechanisms of removing heavy metals and dyes from aqueous solution using date pits solid adsorbent. *J Hazard Mater*. 2010;176(1-3):510-520.

doi: 10.1016/j.jhazmat.2009.11.059

24. Lackmann C, Brendt J, Seiler TB, *et al.* The Green toxicology approach: Insight towards the eco-toxicologically safe development of benign catalysts. *J Hazard Mater*. 2021;416:125889.

doi: 10.1016/j.jhazmat.2021.125889

25. Zamora R, McEvoy J, Colbert C, Chacana Olivares J, Kaewlom P, Khan E. Blocking bacterial appendage attachment to wastewater treatment membranes using anti-adhesins. *Chemosphere*. 2023;323:138246.

doi: 10.1016/j.chemosphere.2023.138246

26. Nouri M. Potentials and challenges of date pits as alternative environmental clean-up ingredients. *Biomass Convers Biorefin*. 2023;13(2):1429-1456.

doi: 10.1007/s13399-020-01215-w

27. Charoenkal K, Yang Z, Wang Z, *et al.* Engineered Zn-enriched biochars for controlled nutrient delivery: Elucidating interfacial mechanisms and mitigating environmental risk. *J Environ Chem Eng*. 2025;13(6):119606.

doi: 10.1016/j.jece.2025.119606

28. Frau F, Atzori R, Ardau C, *et al.* A two-step pH control method to remove divalent metals from near-neutral mining and metallurgical waste drainages by inducing the formation of layered double hydroxide. *J Environ Manage*. 2020;271:111043.

doi: 10.1016/j.jenvman.2020.111043

29. Song X, Zhang Y, Yan C, Jiang W, Chang C. The Langmuir monolayer adsorption model of organic matter into effective pores in activated carbon. *J Colloid Interface Sci*. 2013;389(1):213-219.

doi: 10.1016/j.jcis.2012.08.060

30. Aita SA, Mahmoud R, Hafez SHM, Zaher A. Investigating adsorption of aqueous heavy metals through isotherms and kinetics with Zn-Co-Fe/LDH for remarkable removal efficiency. *Appl Water Sci*. 2025;15(4).

doi: 10.1007/s13201-025-02390-9

31. Buonomenna MG, Mousavi SM, Hashemi SA, Lai CW. Water Cleaning Adsorptive Membranes for Efficient Removal of Heavy Metals and Metalloids. *Water*. 2022;14(17):2718.

doi: 10.3390/w14172718

32. Ho YS, McKay G. Pseudo-second order model for sorption processes. *Process Biochem*. 1999;34(5):451-465.

doi: 10.1016/S0032-9592(98)00112-5

33. Tran HN, You SJ, Hosseini-Bandegharaei A, Chao HP. Mistakes and inconsistencies regarding adsorption of contaminants from aqueous solutions: A critical review. *Water Res*. 2017;120:88-116.

doi: 10.1016/j.watres.2017.04.014

34. Foo KY, Hameed BH. Insights into the modeling of adsorption isotherm systems. *Chem Eng J*. 2010;156(1):2-10.

doi: 10.1016/j.cej.2009.09.013

35. Tan X, Liu Y, Zeng G, *et al.* Application of biochar for the removal of pollutants from aqueous solutions. *Chemosphere*. 2015;125:70-85.

doi: 10.1016/j.chemosphere.2014.12.058